A Robust Fully-Digital Drive for Linear Permanent Magnet Synchronous Motor

Michael S.W. Tam* Norbert C. Cheung**

*ASM Assembly Automation, Watson Centre, 16 Kung Yip St., Kwai Chung, N.T., Hong Kong
**Department of Electrical Engineering The Hong Kong Polytechnic University, Hong Kong
E-mail: *swtam@asmpt.com   **eencheun@polyu.edu.hk

Abstract –High-speed and high-precision linear motions are found in many industrial applications, such as the wire-bonding and die-bonding of microelectronic components [1]. In order to achieve the strict requirements of next-generation semiconductor packaging machines, a high-performance linear drive system is developed. The linear drive system consists of a Linear Permanent Magnet Synchronous Motor (LPMSM), and a DSP-based fully digital PWM drive. To increase the current dynamics, overrated momentary high-voltage and high-current are injected to the actuator's coils, through the PWM drive. Finally, to improve the system robustness, a force compensation loop is derived to attain the system dynamic response when load variation is present. This paper describes the development of such a robust linear drive system. The paper includes (i) the construction and modelling of the Permanent Magnet Synchronous Linear Drive (PMSM); (ii) the design of the robust linear drive and the control system; (iii) the hardware implementation of the linear drive system; and (iv) the implementation results. The final results show that the system is capable of maintaining the same motion dynamic with load variation from 1kg to 2kg.

INTRODUCTION

Linear Permanent Magnet Synchronous Motors (LPMSMs) have inherent advantages of direct drive, zero backlash, simple structure, high thrust density, and almost maintenance free [1, 2, 3]. Therefore it is particularly suitable for linear motion system where high speed and high precision are required. However, it has not gained widespread utilization, due to its non-conventional structure and the difficulty of direct-drive control [1, 6]. Unlike rotary motors, LPMSMs have limited travelling ranges, they usually cannot operate and test under speed control mode [7]. Moreover, the motor has end-effects which need to be considered and modelled [2, 3]. Under direct-drive mode, any disturbance in the load is directly reflected back to the PWM drive and the controller [9, 10, 11]. Therefore, to operate the LPMSM at very high acceleration/deceleration rates and very high accuracy creates certain challenges to the drive designer.

This paper describes the structure of the LPMSM and its modelling method; the PWM current drive and the robust motion controller; and the actual implementation of the drive system.

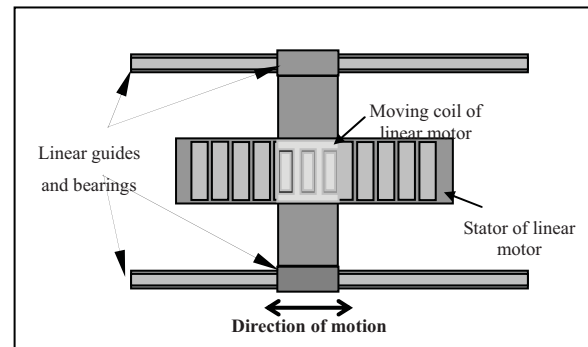## CONSTRUCTION OF THE LINEAR MOTOR AND THE DIGITAL DRIVE

Fig. 1 Structure of direct drive linear motion system

The simplified diagram that illustrates the structure of the direct drive linear motion system is shown in Fig. 1. It is a 3-phase permanent magnet synchronous motor with three separated delta connected moving coils and a magnetic track as the stator.

The simplified cross section of the linear motor is shown in Fig. 2. The magnetic flux density along the stator is designed to be a sinusoidal distributed. For the mover is moving in parallel over the stator in a constant velocity, the EMFs generated across the 3 coils are sinusoidal with 120° phase-shift from each other. The voltage equation for the LPMSM is thus given by (1).
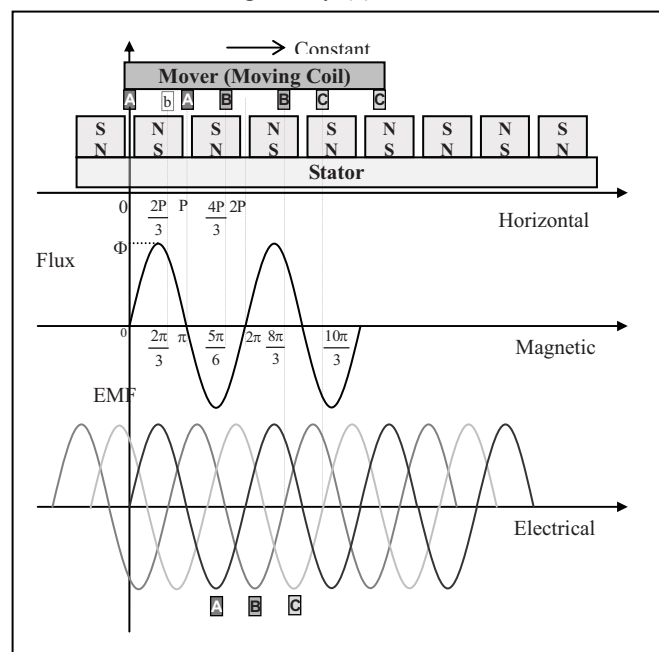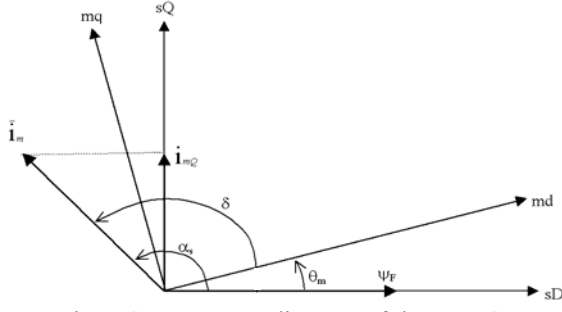

Fig. 2 Side view of the linear motor

Fig. 3 Space vector diagram of the LPMSM

$$
\begin{bmatrix} v_a \\ v_b \\ v_c \end{bmatrix} = \begin{bmatrix} R & 0 & 0 \\ 0 & R & 0 \\ 0 & 0 & R \end{bmatrix} \begin{bmatrix} i_a \\ i_b \\ i_c \end{bmatrix} + \frac{d}{dt}\begin{bmatrix} L & 0 & 0 \\ 0 & L & 0 \\ 0 & 0 & L \end{bmatrix} \begin{bmatrix} i_a \\ i_b \\ i_c \end{bmatrix} + K_e u \begin{bmatrix} \cos\left(\dfrac{ut}{p}\right) \\ \cos\left(\dfrac{ut}{p} - \dfrac{3\pi}{2}\right) \\ \cos\left(\dfrac{ut}{p} + \dfrac{3\pi}{2}\right) \end{bmatrix}
$$

(1)

Assuming that there is a complete electro-mechanical energy transfer, the thrust force produced by the motor is:

$$
F_e = \frac{1}{u}(i_a \mathbf{e}_a + i_b \mathbf{e}_b + i_c \mathbf{e}_c)
$$

(2)

Taking into account the frictional force $B\,u$, the mover's inertia M_M, the cogging force F_C and the load F_L, the mechanical force output is:

$$
F_M = M_M \frac{d}{dt}u + B\,u + F_L + F_C
$$

(3)

where B is the frictional constant of the mover.

STYLE THRUST CONTROL OF THE LINEAR MOTOR

As shown in **Error! Reference source not found.**, the thrust force of the LPMSM is the cross-product of the space vector of the stator magnet flux (ψ_F) and the space vector of the mover current. (I_m). The thrust force can be written as:

$$
T_F = C_F \; \bar{\psi}_F \times \; \bar{i}_m
$$

where C_F is a constant ψ_F is the flux linkage space vector in stator reference frame, i_m is the mover current space vector in stator reference frame

It is therefore the i_{mQ} component of the current space vector of the mover has the effect of producing the electro-magnetic force, and the thrust force is thus:

$$
T_F = C_F \, \psi_F \, i_{mQ} \quad or \quad = C_F \, \psi_F \,/\, \bar{i}_m \!\sin\alpha_S
$$

So the maximum thrust can be obtained when the space-vector of the mover current leads the stator magnet flux of

the direct axis by 90°. The magnetic position of the mover with respect to the stator is monitored by the linear encoder. The block diagram for the thrust control of the LPMSM is shown in **Error! Reference source not found.**.
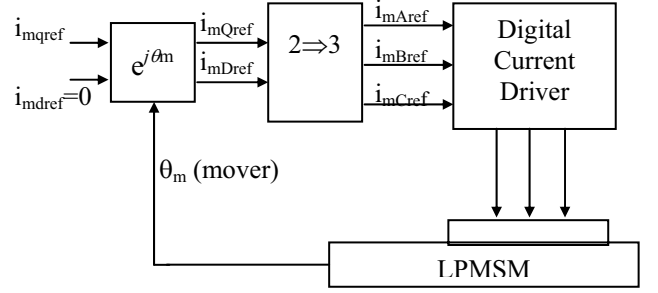

Fig. 4 Thrust control of the LPMSM

A linear incremental encoder is used to monitor the mover position. The mover current components in the stationary reference frame, i_{mQref} and i_{mDref}, are obtained by using the transformation $exp(j\theta_m)$. The actual 3-phase current command for the digital driver is obtained by the application of the 2-phase-to-3-phase transformation [11]. Below is the matrix for the 2-phase-to-3-phase transformation:

$$
\begin{bmatrix} S_a \\ S_b \\ S_c \end{bmatrix} = \begin{bmatrix} \cos\theta_m & \sin\theta_m & 1 \\ \cos(\theta_m - 2/3\pi) & \sin(\theta_m - 2/3\pi) & 1 \\ \cos(\theta_m - 4/3\pi) & \sin(\theta_m - 4/3\pi) & 1 \end{bmatrix}\begin{bmatrix} S_q \\ S_d \\ S_0 \end{bmatrix}
$$

(4)

where θ_m is the mover electrical angle and is equal to ut/p

THE ROBUST FORCE COMPENSATED LINEAR DRIVER SYSTEM

The proposed control strategy for the robust force compensated linear drive system is shown in Fig. 5. The robustness of the system is improved by introducing a force loop into the traditional PID control loop. The software reference load is build which has characteristics matched with the actual motor load. In case that there is no parameters change in the operation environment, the acceleration of the reference and the actual load will be the same. The error feed into the Force control block is zero and no compensation signal is generated.
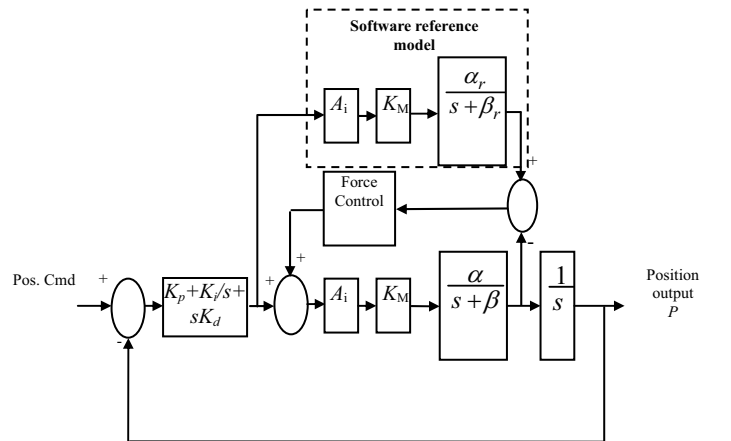

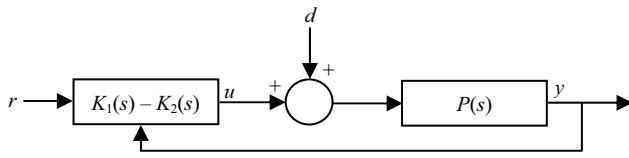Fig. 5 Block diagram of the robust control of the LPMSM
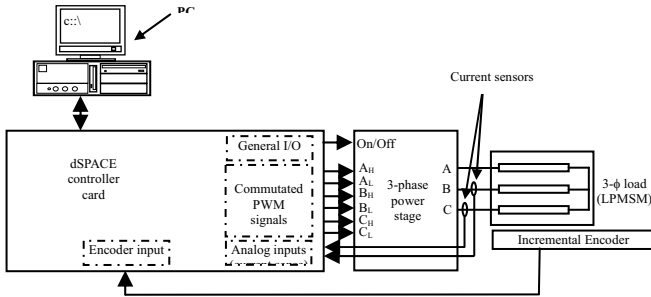
Fig. 1 A general 2DOF controller

Fig. 2 Block diagram of the digital driver

Fig. 3 Block diagram of the digital driver

Fig. 4 Construction of the power drive stage

Fig. 5 The linear PMSM motion system

THE CONTROLLER DESIGN

The feedback system in Fig. 6 is a general two degree of freedom (2DOF) controller. It can be proved the overall system stability can be is sustained if the inner force loop is stable. For any stable system which can even be nonlinear and time varying, the nominal tracking performance is unaffected and the closed loop stability is guaranteed [15, 16].

The function of the force control block is to derive the compensation force from the velocity error input. Therefore the logical transfer function of the block is the inverse function of the software model (i.e. the inverse of the original actual load). In that case the force loop will produce no output as the load has no changes. Otherwise the inverse characteristic of a motor load will transform the velocity error signal to a compensation force to drive the actual load to the original desired response. A low pass filter is added to the force loop in order to filter the noise pick-up and avoid instant feedback that may drive the power drive to saturation.

The transfer function for the Force Compensation Controller Fc is:

$$F_C = \frac{s + \beta_r}{K_f s + \alpha_r} \qquad (5)$$

where K_f is to select the low pass characteristic of the force compensation control controller

HARDWARE IMPLEMENTATION OF THE DRIVE SYSTEM

To reduce the development time, the Real-Time Workshop toolbox of the Matlab software is used for generating the software code of the control algorithm of the model direct to the dSPACE controller card DS1102. The DS1102 controller card provides powerful interface and processing power for easy implementation of the required control system.
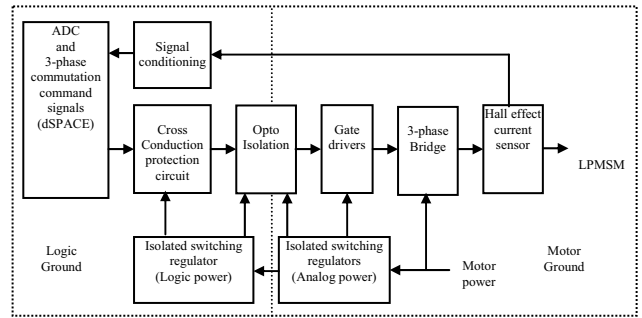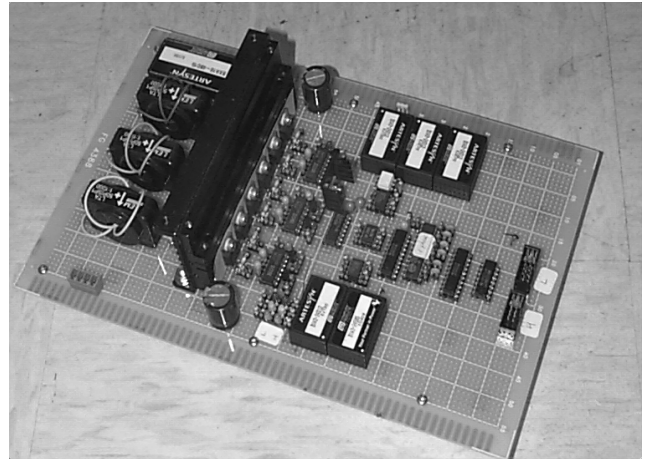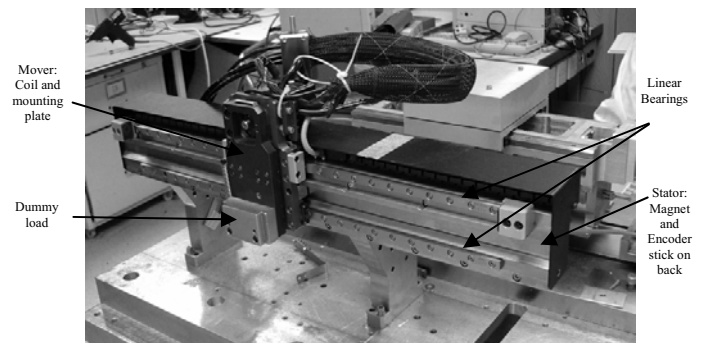
The arrangement of the parts for the digital LPMSM driver is shown in the Fig. 7. It consists of a PC for editing, compiling, monitoring and downloading the program into the dSPACE card. The dSPACE card is the controller that contains a DSP, I/O, PWM outputs and Analog input for controlling the 3-phase driver. The 3-phase driver is for delivering power to the linear motor whose current is to be controlled.

The block diagram of the digital driver is as shown in Fig. 8. It consists of a PC and a DS1102 dSPACE card serves as the current controller. Hall effect current sensors and the signal conditioning circuit give a feedback full scale of 10V to the dSPACE ADCs at 12A full current output. The 100KHz bandwidth of the Hall effect current sensors

ensure a sufficient signal dynamic for a 1KHz close-loop current response.

The power stage consists of three half-bridge of power MOSFET. The 3-phase power bridges are driven by three half bridges and a GAL22V10 chip are used for deriving the six PWM signals for the gate drivers. An addition of 400nS dead time is also introduced by associated RC network, which gives an overall minimum dead time of 800nS.

The construction of the power driver stage and LPMSM of the linear motion system is shown in Fig. 9 and Fig. 10. Since all the current and trajectory control functions are implemented digitally, the overall hardware is not very complicated. The LPMSM has an effective travelling distance of 30cm, and can produce a thrust of 139N at a peak vector current of 12A.
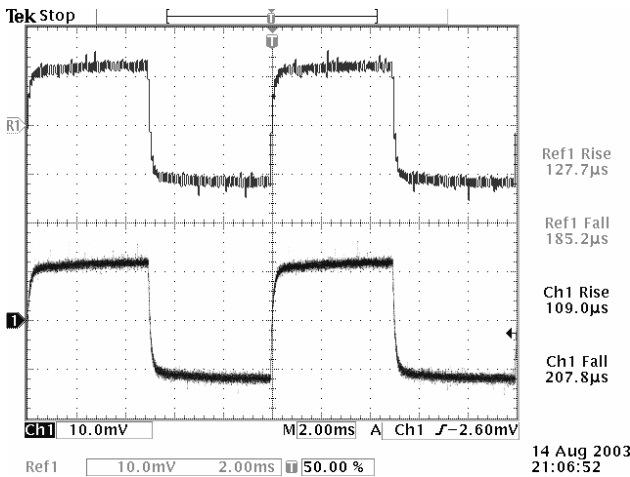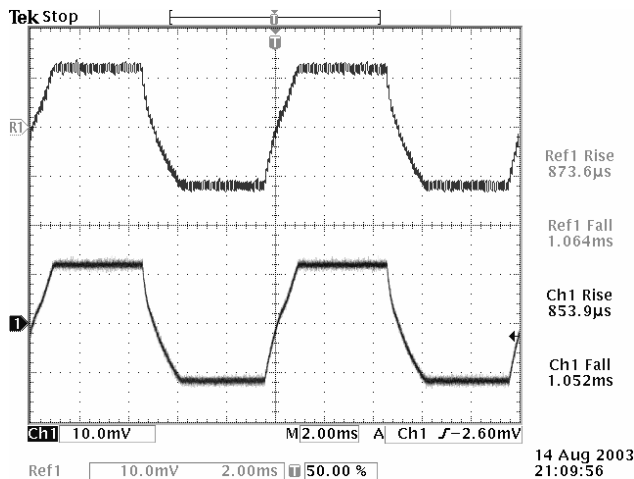

Fig. 6 10% current loop step response

Fig. 7 100% current loop step response

TEST RESULTS

The actual small current step responses, which are 10% of the maximum, of two of the phases of the LPMSM driver are shown in Fig. 11. The full load current step response is shown is in Fig. 12. These results show that the current profile can track the command current closely in small and full load conditions. Small signal rise/fall time of about 0.2ms is measured while about 1ms for the large signal

responses. The actual motion responses of the LPMSM drive system are shown in Fig. 13 to Fig. 17.
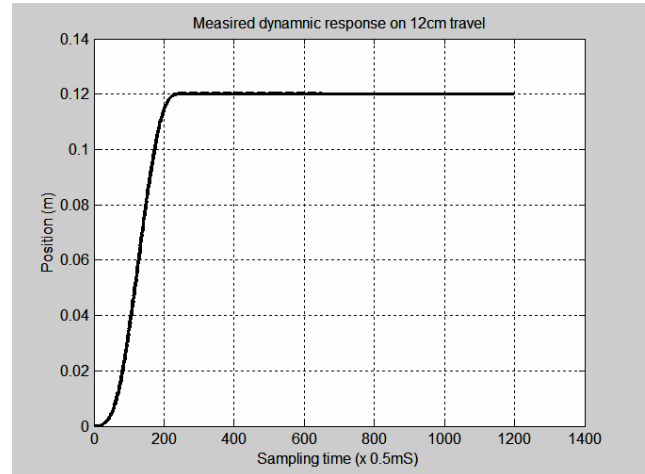

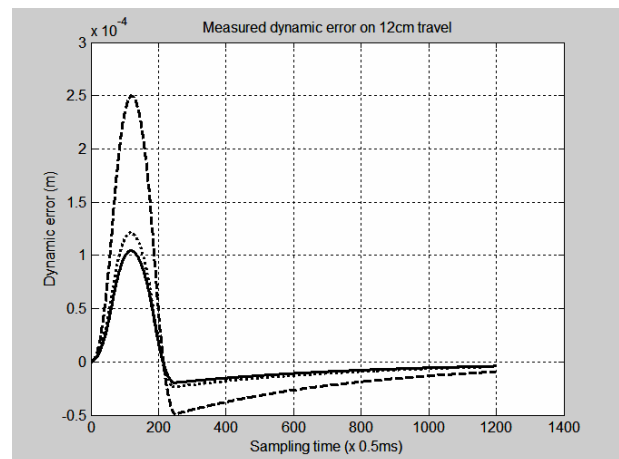Fig. 8 Actual dynamic response of the robust LPMSM drive system

Fig. 9 Measured dynamic error

The measured dynamic response of the LPMSM drive system is shown in Fig. 13. The 2kg load with no force compensation exhibits some overshoot. The solid curves are the responses of traditional PID controller with no force compensation. The dashed curves are the responses of the traditional PID position controller when load is changed from 1kg to 2kg with no force compensation. The dotted curves are the 2kg load response with force compensator activated. All the three responses are similar and the position dynamics are close to each others. The overshoot for 1kg load response is 0.17%. The overshoots with and with no force compensation is 0.21% and 0.42% respectively.

The measured dynamic error is shown in Fig. 14. In the 1kg load response, the peak error and time to settle within 15m are 110m and 200ms (400 sampling time) respectively. When the load is changed from 1kg to 2kg and force compensation is not activated, the dynamic error is increased from a peak error of 110m to 250m. The settling time is increased to 460ms. When the force compensator is activated, the peak dynamic error drops to 120m and is closed to the 1kg response. With the force compensator, the settling time for the error to fall within 15m is 250ms (500 sample time).
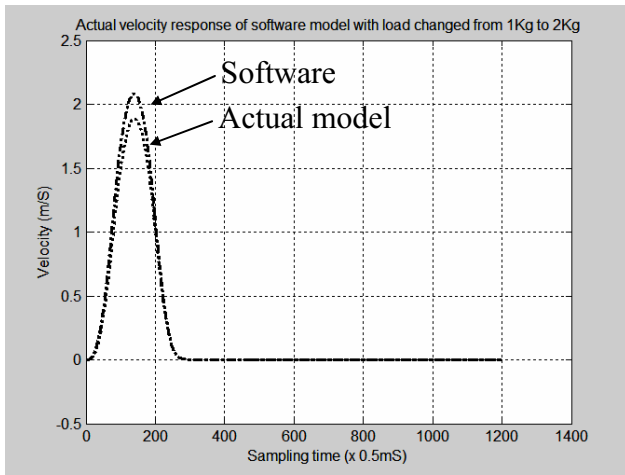
191

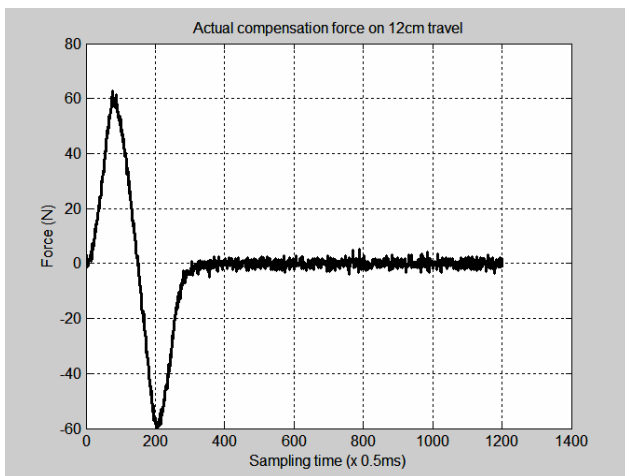Fig. 10 Measured velocity of software and actual model
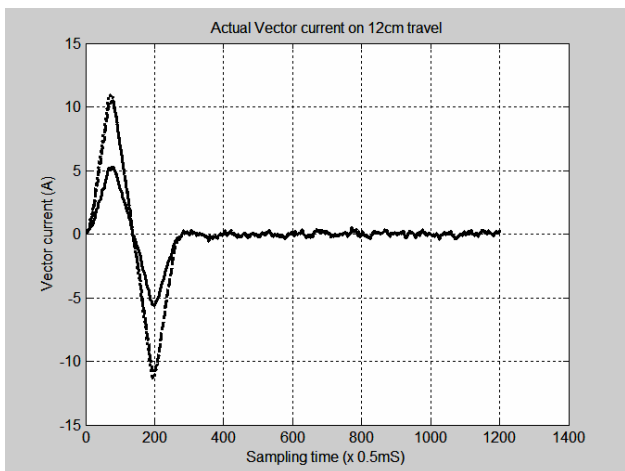

Fig. 11 Actual output of force compensator

Fig. 12 Actual vector current

The measured velocity responses of the software motor model and the actual motor model with force compensation are shown in Fig. 15. The velocity profile of the actual model is lower than the software model when the load is increased from 1kg to 2kg. The peak velocity difference is 2.08m/S - 1.89m/s = 0.19m/s. The corresponding output of the force compensator is shown Fig. 16. The force compensator produces a peak correcting force of 60N to minimize the velocity difference between the actual and software model.

The measured vector current responses are shown in Fig. 17. Both the vector current profiles are similar for the 2kg load response. When the force compensator is not activated, the peak current is increased from 5.3A to 10.5A. If the force compensator is activated, the vector current is increased to 10.9A. The activation of force compensator has an effect to advance the vector current.

The measured results are summarized in Table 1. An accuracy of about 10m steady state error and an acceleration of 6G are measured.

CONCLUSION

This paper describes the development of a linear drive system with high-acceleration/deceleration and high accuracy performances. A fully digital PWM circuit that supplies momentary over-rated current to the LPMSM is constructed. A robust controller with force compensation loop is proposed. The overall system is simulated and implemented in hardware. Both simulated results and implementation measurements show that the current controller has a fast current loop response and good current tracking ability. The system has been compared with the tradition PD controller. It is demonstrated that the control system is able to maintain a consistent dynamic error in response to a load change of 1kg to 2kg. The developed linear drive system is very suitable for deployment in next-generation of high-performance electronic packaging machines.

	1kg load	2kg load	2kg load
Force compensation	-	No	Yes
% overshoot	0.17%	0.42%	0.21%
Peak dynamic error	110μm	250μm	120μm
Settling time (within 15μm)	200ms	460ms	250ms
Peak vector current	5.3A	10.5A	10.9A
Peak velocity	1.925m/s	1.928m/s	1.89m/s
Peak acceleration	6.1G	5.95G	6G
Peak compensation force	-	-	62N

Table 1 Measured results summary

the achievement in this section. The following statement is an example: The theory has been implemented in an electronic circuit. The circuit has been prototyped and tested. The experimental results agreed very well with the theoretical prediction and verified the theory proposed.

REFERENCES

[1] J. F. Gieras and M. Wing, Permanent Magnet Motor Technology: Design and Application, Marcel Dekker, Inc., 2002.

[2] S. R. Trout, "Material selection of permanent magnet, considering thermal properties correctly", Proc. on Electrical Electronics Insulation Conference and Electrical Manufacturing & Coil Winding Conference, pp.365-370 Oct. 2001.

[3] J. F. Gieras and Z. J. Piech, Linear Synchronous Motors: Transportation and Automation Systems, CRC Press, 2000.

[4] I. Boldea and S. A. Nasar, Linear Electric Actuators and Generators, Cambridge University Press, 1997.

[5] D. W. Novotny and T. A. Lipo, Vector Control and Dynamics of AC Drives, Oxford Science Publications, 1998.

[6] J. S. Ko, J. H. Lee and M. J. Youn, "Robust digital position control of brushless DC motor with adaptive load torque observer," IEE Proc. Electr. Power Appl., vol.141, no.2, Mar. 1994.

[7] M. S. W. Tam and N. C. Cheung, "A high-speed, high-precision linear drive system for manufacturing automations," APEC 2001 Conference Proceedings, vol. 1, no.13A4, Mar.2001.

[8] M. S. W. Tam, N. C. Cheung, "An all-digital high performance drive system for linear permanent magnet synchronous motor," CPSC 2001 Conference Proceedings, vol. 14, pp.321, Sept 2001.

[9] W. C. Gan and L. Qiu, "Design and analysis of a plug-in robust compensator: an application to indirect-field-oriented-control induction machine drives," IEEE Trans. on Industrial Electronics, vol. 50, no. 2, pp.272-282, Apr. 2003.

[10] K. Zhou, J. C. Doyle and K. Glover, Robust and Optimal Control, Prentice Hall, 1996.

[11] K. Zhou and J. C. Doyle, Essentials of Robust Control, Prentice Hall, 1998.

[12] K. Zhou and Z. Ren, "A new controller architecture for high performance, robust, adaptive, and fault tolerant control," IEEE Trans. on Automatic Control, vol. 46, no. 10, pp. 1613-1618, Oct. 2000.

[13] J. O. Krah and J. Holtz, "High performance current regulation and efficient PWM implementation for low-inductance servo motors," IEEE Trans. on Industry Applications, vol. 35 issue: 5, pp. 1039-1049, Sep.-Oct. 1999.

[14] M. Vidyasagar, Control System Synthesis, The MIT Press, Cambrigde, 1985.

[15] P. P. Khargonekar and K. R. Poolla, "Uniformly optimal control of linear time-invariant plants: nonlinear time-varying controllers," System and Control Letters, vol. 6, no. 5, pp. 3003-308, 1986.

[16] K. Zhou and Z. Ren, "A new controller architecture for high performance, robust, adaptive, and fault tolerant control." IEEE Trans. Automation Control, vol. 46, no. 10, pp. 1613-1618, Oct. 2000.